ICSV13 - Vienna

The Thirteenth International Congress on Sound and Vibration

Vienna, Austria, July 2-6, 2006

# QUANTITATIVE AND QUALITATIVE VERIFICATION OF PRESSURE AND VELOCITY BASED PLANAR NEAR-FIELD ACOUSTIC HOLOGRAPHY

Rick Scholte, Ines Lopez, and Bert Roozen

Mechanical Engineering, Eindhoven University of Technology
P.O. Box 513, 5600 MD Eindhoven, The Netherlands
r.scholte@tue.nl

## Abstract

Planar Near-field Acoustic Holography (PNAH) is nowadays implemented at various companies and institutes. At all times, seemingly correct acoustic images are created that are treated accordingly. Caution has to be taken while interpreting these results, since incompetent windowing and filter implementation leads to results that are far from the exact solution. In order to avoid certain cases and probable misinterpretations, a number of recent developments were made. A significant part of the most recent developments are discussed shortly, followed by an in-depth comparison and verification of results, based on both sound pressure and particle velocity measurements.

Various anti-leakage windowing techniques will be discussed and compared. Border-padding is compared to classical windowing on larger grid sizes. Sound pressure and particle velocity measurements on various distances on a stationary spinning hard disk are used to obtain inverse solutions. Also, multiple distances are measured and compared to the obtained inverse solutions. The flat top cover of the hard disk is scanned by a traversed laser vibration system. These velocities of the cover are compared to inverse solutions of the particle velocity at the source plane, where both sound pressure and particle velocity are used to obtain these results. This makes it possible to quantitatively compare pressure to velocity and velocity to velocity PNAH.

## INTRODUCTION

The use of Fourier Transforms in acoustic imaging is very beneficial in terms of processing speed and complexity, while it provides a very accurate solution to the inverse solution of the wave equation. On the other hand, application of the Fourier Transform requests a thorough knowledge of sampling theory and requirements for proper transforms. In theory inverse acoustic problems are accurate and some even

exact in continuous forms, but in practise we deal with finite measurement grids with discrete spatial sampling, acoustic sensors and measurement systems which introduce noise, distortion and certain boundaries. These practical factors should not be ignored and play an important role for inverse acoustic methods to be successful.
In the following, a well-known technique developed in the 80's of last century, PNAH [1], is discussed, with some thoughts and tools to deal with more practical aspects and possible errors. These will be illustrated by a practical case with particle velocity and sound pressure measurements on an operational hard disk. The results after solving the inverse problem are compared to laser vibrometer measurements.

## THEORETICAL OUTLINE

### Pressure and Velocity Based Planar Near-field Acoustic Holography

PNAH is characterized by the use of the spatial frequency domain, or k-space, in order to obtain the inverse solution of the wave equation. In k-space a relatively easy solution for the inverse problem of complex sound pressure or particle velocity at a distance $z_h$ (hologram plane) to an arbitrary distance $z$ can be obtained. The boundary condition for the distance $z$ is $z \geq 0$, where the half-space $z < 0$ is defined as the source space. Outside the source space sound sources are not allowed. This means we can calculate sound pressure and particle velocity at an infinite number of planes parallel to the source plane $z = z_s = 0$, in between $z_h$ and $z_s$. From [2] it follows that

$$\hat{\hat{p}}(k_x, k_y, z, \omega) = \hat{\hat{p}}(k_x, k_y, z_h, \omega) \cdot e^{jk_z(z-z_h)}, \quad (1)$$

by using Euler's equation the particle velocity in normal direction $\hat{\hat{v}}_z(k_x, k_y, z, \omega)$ can be determined from the sound pressure in k-space:

$$\hat{\hat{v}}_z(k_x, k_y, z, \omega) = \hat{\hat{p}}(k_x, k_y, z_h, \omega) \cdot \frac{k_z}{\rho c_0 k} e^{jk_z(z-z_h)}, \quad (2)$$

The part after $\hat{\hat{p}}(k_x, k_y, z_h, \omega)$ in both (2) and (3) is generally called upon as the inverse propagator. As a matter of fact, given these equations it is possible to determine all inverse propagators when either $\hat{\hat{p}}(k_x, k_y, z_h, \omega)$, $\hat{\hat{v}}_x(k_x, k_y, z_h, \omega)$, $\hat{\hat{v}}_y(k_x, k_y, z_h, \omega)$, or $\hat{\hat{v}}_z(k_x, k_y, z_h, \omega)$ is known. All inverse propagators for given in- and output quantities are shown in a table in Figure 1. The inverse propagators are arced in grey cells with thick borders, and are multiplied with the hologram quantities shown above these cells to obtain the required acoustic quantities at a distance $z$ corresponding to the cells shown to the left of the inverse propagators.

From a practical point of view, the k-space counterparts at $z_h$ can only be obtained by measuring sound pressure or particle velocity at a discrete number of positions in a bounded plane. This is where the trouble starts. It is generally known that frequency analysis of a time signal of limited length, at a certain sampling rate requires proper anti-aliasing and anti-leakage filters in order to be useful. The same holds for PNAH in spatial versus wavenumber domain analysis. The spatial pre-processor block contains spatial anti-leakage and padding functions that render the data suitable for 2-dimensional Fast Fourier Transform (2D FFT). Spatial sampling and aliasing, spatial pre-processing and low-pass filtering will be discussed below.

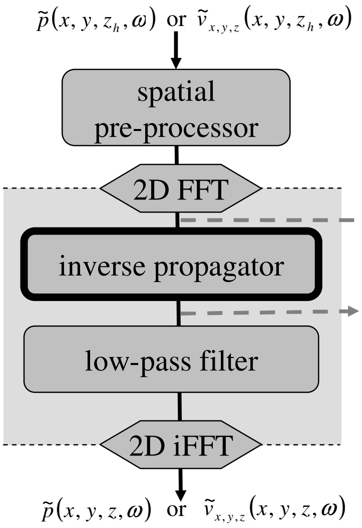


example: $\hat{\tilde{v}}_z(k_x, k_y, z, \omega) = \hat{\tilde{p}}(k_x, k_y, z_h, \omega) \cdot \boxed{\frac{k_z}{\rho c_0 k} e^{jk_z(z-z_h)}}$

**i-propagator**

| | $\hat{\tilde{p}}(k_x,k_y,z_h,\omega)$ | $\hat{\tilde{v}}_x(k_x,k_y,z_h,\omega)$ | $\hat{\tilde{v}}_y(k_x,k_y,z_h,\omega)$ | $\hat{\tilde{v}}_z(k_x,k_y,z_h,\omega)$ |
|---|---|---|---|---|
| $\hat{\tilde{p}}(k_x,k_y,z,\omega)$ | $e^{jk_z(z-z_h)}$ | $\frac{\rho c_0 k}{k_x} e^{jk_z(z-z_h)}$ | $\frac{\rho c_0 k}{k_y} e^{jk_z(z-z_h)}$ | $\frac{\rho c_0 k}{k_z} e^{jk_z(z-z_h)}$ |
| $\hat{\tilde{v}}_x(k_x,k_y,z,\omega)$ | $\frac{k_x}{\rho c_0 k} e^{jk_z(z-z_h)}$ | $e^{jk_z(z-z_h)}$ | $\frac{k_x}{k_y} e^{jk_z(z-z_h)}$ | $\frac{k_x}{k_z} e^{jk_z(z-z_h)}$ |
| $\hat{\tilde{v}}_y(k_x,k_y,z,\omega)$ | $\frac{k_y}{\rho c_0 k} e^{jk_z(z-z_h)}$ | $\frac{k_y}{k_x} e^{jk_z(z-z_h)}$ | $e^{jk_z(z-z_h)}$ | $\frac{k_y}{k_z} e^{jk_z(z-z_h)}$ |
| $\hat{\tilde{v}}_z(k_x,k_y,z,\omega)$ | $\frac{k_z}{\rho c_0 k} e^{jk_z(z-z_h)}$ | $\frac{k_z}{k_x} e^{jk_z(z-z_h)}$ | $\frac{k_z}{k_y} e^{jk_z(z-z_h)}$ | $e^{jk_z(z-z_h)}$ |

**i-propagators**

Figure 1: PNAH step-wise process (left); table with inverse propagators (right), depending on input (measured) data an inverse propagator can be chosen to calculate the required acoustical quantity.

## Spatial Sampling and Pre-processing

Measurements with acoustic sensors in space can be explained as spatial sampling of acoustic properties. In [3] we have stated an inequality that shows how to apply a natural anti-aliasing filter:

$$\sqrt{k^2 + \left(\frac{D \cdot \ln 10}{20(z_h - z_s)}\right)^2} > 0.5 \cdot k_{sample} . \quad (3)$$

The possibility exists that aliasing occurs when this inequality is true. It tells us that under certain noise conditions the measurement distance can be too small given the chosen inter-sensor distance.

Another problem is leakage. The finiteness of the hologram measurement grid introduces a certain wavenumber detail $\Delta k_x$ for a given width of the total grid $X$ by $\Delta k_x = 2\pi / X$ in [$radm^{-1}$]. To reduce leakage, spatial windowing is to be applied before transforming the data to k-space by means of a 2D FFT. A downside of windowing is the deterioration of a large part of the hologram data, which results in serious errors at the source. A way of avoiding these errors is a recently introduced technique called border-padding [4], which uses the pressures or particle velocities at the grid border and pads these outward. A carefully applied window minimizes the modification of the measured data. Although it adds non-physical data outside the hologram, the resulting effects are cut off at the end of the PNAH process, after inverse 2D FFT.

**Low-pass Filtering and L-curve**

A well-known issue with inverse problems is the blow-up of noise in the hologram. The noise at high wavenumbers should be suppressed, but first some insight in k-space is required.
From Figure 1 it follows that we need to determine $k_z$ from the wavenumbers in both x- and y- direction, i.e. $k_x$ and $k_y$, and the acoustic wavenumber $k$ that follows from $\omega$ and $c_0$. In k-space $k_z$ is determined by $k_z = \pm\sqrt{k^2 - k_x^2 - k_y^2}$ of which three types of solutions to this equation, with $k$ already known, can be found:

$$\begin{aligned} &k_x^2 + k_y^2 = 0 && \textbf{a}\text{: plane wave in z-direction} \\ &0 < k_x^2 + k_y^2 \le k^2 && \textbf{b}\text{: propagating waves; } k_z \text{ is real} \\ &k_x^2 + k_y^2 > k^2 && \textbf{c}\text{: evanescent waves; } k_z \text{ is complex} \end{aligned} \tag{4}$$

The radiation circle lies exactly at $k^2 = k_x^2 + k_y^2$ and is noted as $k_r$, outside this circle waves are evanescent, whereas inside waves are propagating. Applying (2) to propagating waves (4a and b) result in a phase shift, evanescent waves (4c) are multiplied in k-space by an exponential power of increasing strength with increasing $k_z$.
From the above follows that noise at higher wavenumbers have a much higher influence on the result compared to noise within the radiation circle. Above a certain wavenumber, noise will dominate the inverse solution. However, information at high wavenumbers results in high spatial detail and thus the ability to identify small sources.
A way to discriminate between high wavenumbers, polluted with noise and useful information at somewhat lower, evanescent and propagating waves is to apply a low-pass, cosine tapered low-pass filter.

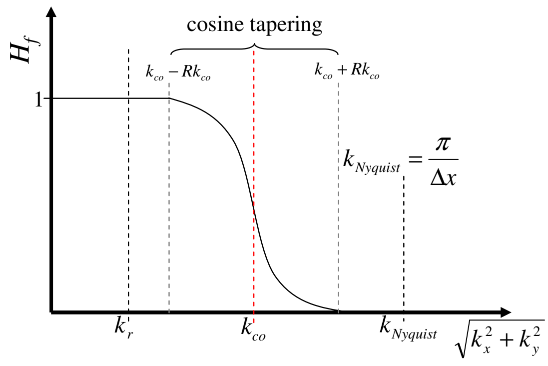


Figure 2: low-pass cosine tapered filter

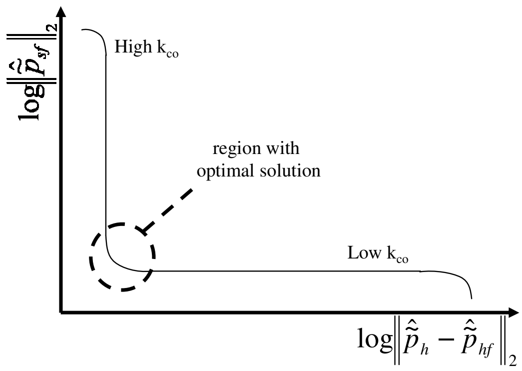


Figure 3: PNAH L-curve by increasing $k_{co}$

The cosine tapering of the applied low-pass wavenumber filter is defined as

$$H_f = \frac{1}{2} + \frac{1}{2}\cos\left(k - \frac{(k_{co} - k_{co}R)}{2k_{co}R}\pi\right),$$
$$for \quad (k_{co} - k_{co}R) \le \sqrt{k_x^2 + k_y^2} \le (k_{co} + k_{co}R). \tag{5}$$

The cosine tapering width is determined by ratio $R$ with respect to $k_{co}$ is chosen. Both $R$ and $k_{co}$ are determined by an iterative process. Step-wise increasing $k_{co}$ will eventually cause blow-up of the solution, on the other hand too much filtering will result in a low-detail result. If we plot the solution norm of the sound pressure,

$$\left\|\hat{\tilde{p}}_{sf}\right\|_2 = \left\|\hat{\tilde{p}}(k_x, k_y, z_s, \omega)\right\|_2, \tag{6}$$

versus the residual norm of unfiltered $\hat{\tilde{p}}_h$ and filtered $\hat{\tilde{p}}_{hf}$ at the hologram plane,

$$\left\|\hat{\tilde{p}}_h - \hat{\tilde{p}}_{hf}\right\|_2 = \left\|\hat{\tilde{p}}(k_x, k_y, z_h, \omega) - H_f(k_x, k_y)\hat{\tilde{p}}(k_x, k_y, z_h, \omega)\right\|_2, \tag{7}$$

a L-curve as shown in Figure 3 results. Note that this process is valid for all inverse solutions of both sound pressure and particle velocity as given in Figure 1.

### “Sinc-effect” Caused by Low-pass Filter

Ideally a low-pass filter passes all wavenumbers below $k_{co}$ and halts all wavenumbers above. In very specific situations, like modal patterns in plates, a low-pass boxcar filter (infinitely steep) results in a good reconstruction, but in practise this type of filter will result in distortion of the result. To illustrate possible problems with this type of filter a 1D example is shown in Figure 4. The FFT of a point-like source contains energy over a wide k-space band, a sudden interruption of this pattern will result in a ringing or “sinc-effect” emerging from the original position of the point-like source after inverse FFT.

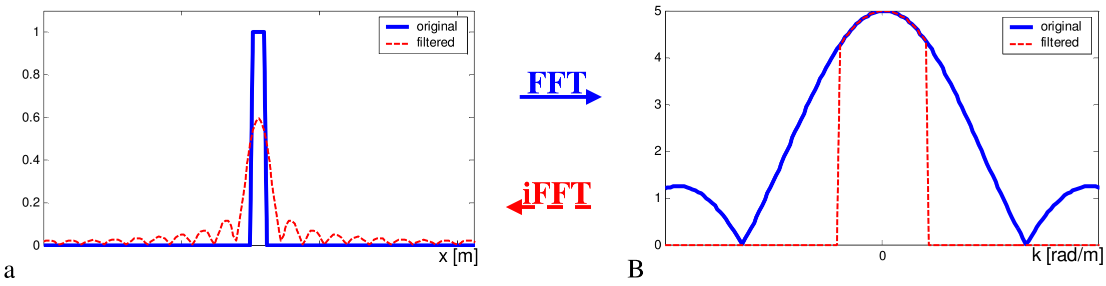


Figure 4: a) point-like source and filtered result (dashed line); b) k-space of both signals

# PRACTICAL STUDY OF HARD DISK ACOUSTICS

## Measurement Setup

The measured source is a Quantum Fireball LCT10 hard disk, mounted in a vertical position with the top cover facing forward, driven in idle mode. The three sensors are placed on a triple axis xyz-robot. The sensors are traversed to pre-defined measurement grid points which, combined, result into holograms of sound pressure and acoustic particle velocity and a surface velocity area scan by the laser.
Sound pressure is measured by a Sonion 8002 that is generally used in hearing aids, the particle velocity is measured by a Microflown [6] placed in normal direction to the hard disk surface, and the laser vibrometer is a Polytec OFV 3000. The measured equidistant grid measures 21 rows by 17 columns with 1cm inter-sensor distance. The laser measurement measures only 13 by 9 points with 1cm spacing since it requires the reflecting area of the hard disk top cover.

## Quantitative and Qualitative Analysis of Results

From a range of peak frequencies from the spectrum, a random frequency of f=1075Hz (k=19.7rad/m) is picked out to verify the results of determining the inverse solution by means of PNAH. Figure 5 shows the PNAH results for measured sound pressure and particle velocity in normal direction, both at 4 and 2cm distance from the hard disk surface. When comparing these results to the laser vibrometer measurements plotted on the right of Figure 5 we see clear similarity between the results. Especially PNAH inputs measured with microphone at 2cm and microflown at 2 and 4cm show a highly similar source pattern compared to the laser. Only PNAH input from microphones at 4cm performs considerably worse.
Worth mentioning is the fact that the low-pass filter for PNAH with microflown measurements has a nearly two-times higher $k_{co}$ than comparable microphone measurements, implicating that the particle velocity hologram contains less noise.
A second interesting result is shown in Figure 6 at f=9669Hz (k=177rad/m), here a point-like source is present exactly on the axis of the disks.

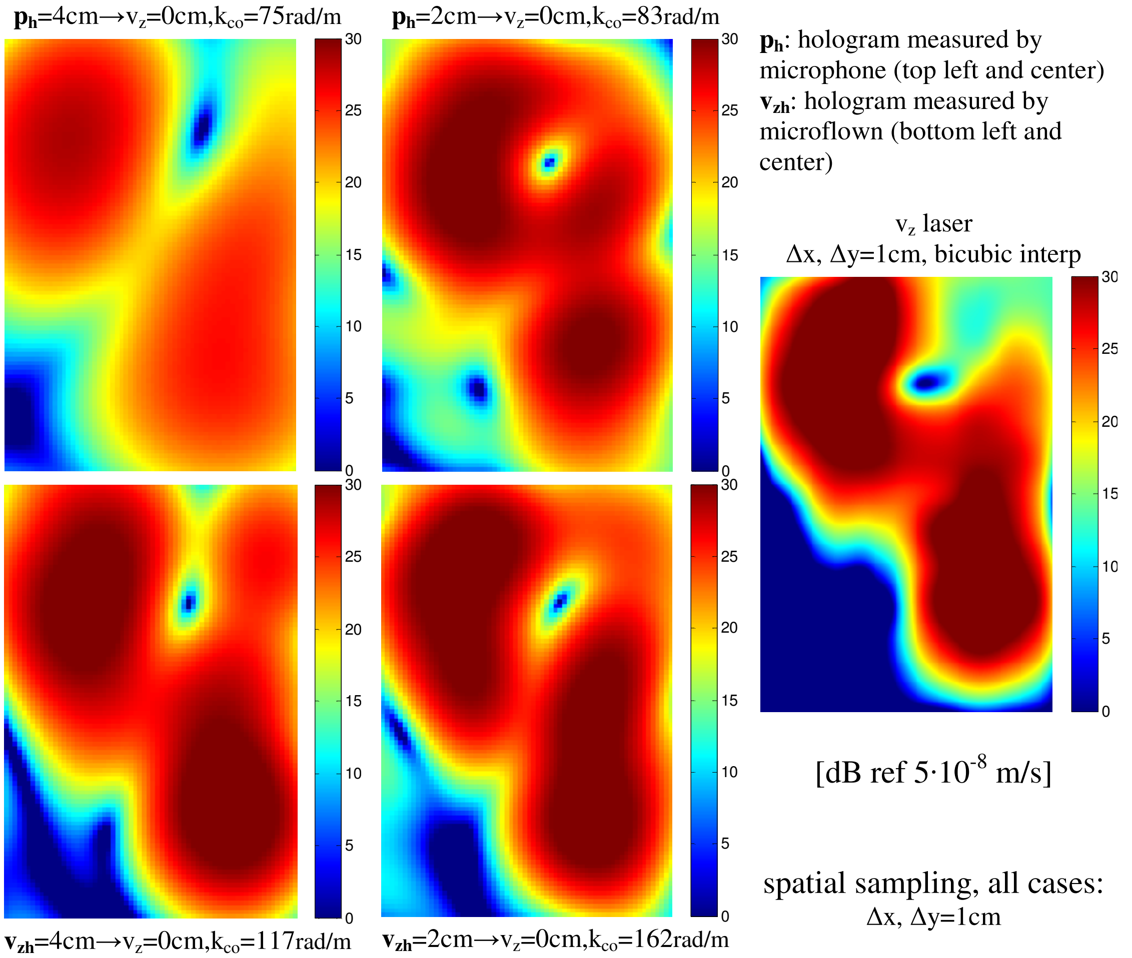


Figure 5: Comparison of holography results at f=1075Hz (k=19.6rad/m), particle velocity at the source plane is compared to laser vibro measured surface velocity

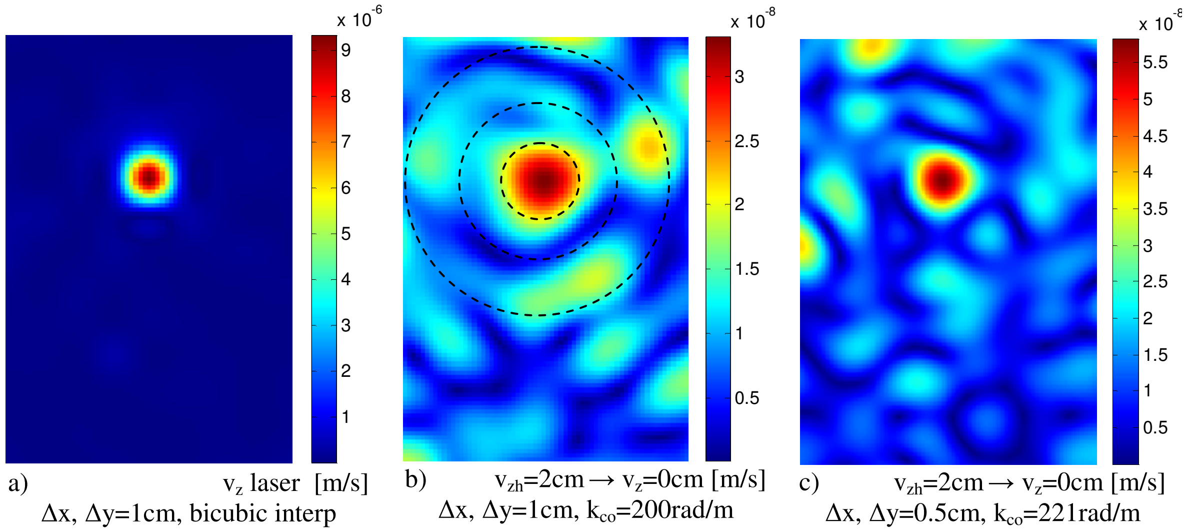


Figure 6: Results of laser vibrometer compared to PNAH of microflown measurements at 2cm from the source at f=9669Hz (k=177rad/m), only spatial sampling (Δx, Δy) and low-pass filters differ

Since this source is present at a relatively high frequency, the wavelength of about 3.5cm is only sampled about 3 times per spatial period with $\Delta x$ =1cm, which is only just above the Nyquist rate. In between $k_r$ and $k_{Nyquist} = \pi / \Delta x$ lies $k_{co}$ and this leaves hardly any k-space to apply a proper cosine tapering of the low-pass filter, resulting in a steep descent and ringing or “sinc-effect” as discussed above. At 1cm spatial sampling as shown in Figure 6b) the typical rings surrounding the source (marked by dashed circles) can be observed although some noisy behaviour is affecting clarity. According to our hypothesis a double spatial sampling rate should attenuate this effect, which clearly shows from the results at 0.5cm spatial sampling in Figure 6c). Also a better quantitative solution for the point source is now found.

## SUMMARY AND DISCUSSION

Since PNAH solves the inverse problem in k-space it requires a rich k-space, yet discretizing the spatial domain by measuring a limited grid with sensors results in a less rich k-space. When pushing the limits of PNAH by measuring point-like sources at high frequencies, with low spatial sampling, errors will occur. This clearly shows the downside of using k-space for inverse problems.
However, when the limits of PNAH are carefully avoided and proper post-processed techniques are applied, accurate results comparable to laser measurements are met. Also, particle velocity to particle velocity PNAH appears to show better results at larger hologram distances. Although a more thorough investigation should be carried out to verify this, since it only shows for this particular case.

## ACKNOWLEDGEMENTS

This work has been performed within the framework of project TWO.6618 of the Dutch Technology Foundation (STW).

## REFERENCES

[1] Maynard J.D., Williams E.G., Lee Y., “Nearfield acoustic holography: I. Theory of generalised holography and the development of NAH”, J.Acoust. Soc. Am., **78 (4)** (1985)

[2] Williams E.G., *Fourier Acoustics. Sound Radiation and Nearfield Acoustical Holography* (Academic Press, 1999)

[3] Scholte R., Roozen N.B., Lopez I., “On spatial sampling and aliasing in acoustic imaging”, 12th Intern. congress on sound and vibration, Lisbon, Portugal (2005)

[4] Scholte R., Roozen N.B., “Improved data representation in NAH applications by means of zero-padding”, 10th Intern. congress on sound and vibration, Stockholm, Sweden (2003)

[5] Scholte R., Roozen N.B., Lopez I., “Regularization in PNAH by means of L-curve”, Forum Acusticum 2005; Budapest, Hungary (2005)

[6] de Bree H-E, “The Microflown, an acoustic particle velocity sensor”, Australian Acoustics, **31(3)** (2003)